Chin. Sci. Bull. (2014) 59(28):3669–3675
DOI 10.1007/s11434-014-0508-y

csb.scichina.com
www.springer.com/scp

Article

Engineering Thermophysics

Anomalies in mid-high-temperature linear thermal expansion coefficient of the closed-cell aluminum foam

Hong Ye · Mingyang Ma · Jilin Yu

Received: 19 August 2013 / Accepted: 3 December 2013 / Published online: 8 July 2014

Abstract Low-density closed-cell aluminum foam is promising to be used as load-bearing and thermal insulation components. It is necessary to systematically study its thermal expansion performance. In this work, linear thermal expansion coefficient (LTEC) of the closed-cell aluminum foam of different density was measured in the temperature range of 100–500 °C. X-ray fluorescence was used to analyze elemental composition of the cell wall material. Phase transition characteristics were analyzed with X-ray diffraction and differential scanning calorimetry. LTEC of the closed-cell aluminum foam was found to be dominated by its cell wall property and independent of its density. Particularly, two anomalies were found and experimentally analyzed. Due to the release of the residual tensile stress, the LTEC declined and even exhibited negative values. After several thermal cycles, the residual stress vanished. With temperature higher than 300 °C, instantaneous LTEC showed hysteresis, which should result from the redistribution of some residual hydrogen in the $Ti_2Al_{20}Ca$ lattice.

Keywords Aluminum foam · Thermal expansion · Residual stress · Phase transition · Hydride · Hysteresis

H. Ye (✉) · M. Ma
Department of Thermal Science and Energy Engineering, University of Science and Technology of China, Hefei 230027, China
e-mail: hye@ustc.edu.cn

J. Yu
Department of Modern Mechanics, University of Science and Technology of China, Hefei 230027, China

1 Introduction

Due to the particular mechanical, thermal, electric and acoustic properties [1–3], metallic foams are drawing increasing attention from both the academic and industrial fields. A lot of works discussed the dependence of the mechanical properties on the structural parameters [4–8] and properties of the cell wall material [9, 10]. It has been revealed that the closed-cell aluminum foam has excellent mechanical properties, especially the energy absorption characteristic. Besides, efforts were made to simulate the heat transfer process based on either regular geometries [11, 12] or CT images [13–15], and the effective thermal conductivity was measured with different methods [16–19]. The closed-cell aluminum foam has been found to have low thermal conductivity and can be used in thermal insulation. Lu et al. [11] and Lázaro et al. [20] reveal that closed-cell aluminum foam shows good fire retardance performance at high temperature. In summary, the closed-cell aluminum foam is promising to be used in some mid-high-temperature situations, acting as load-bearing and thermal insulation components. In such situations, the thermal expansion coefficient affects the magnitude and distribution of thermal stress and strain. So it is extremely important to systematically study the thermal expansion behavior of the closed-cell aluminum foam.

However, work on thermal expansion behavior of the closed-cell aluminum foam is seldom reported. Using a continuum micromechanical model, Kitazono et al. [21] reveals that LTEC of the closed-cell aluminum foam is equal to that of the cell wall material and independent on its density. Based on Voronoi model, Hosseini et al. [22] finds that LTEC of the closed-cell aluminum foam is related to neither density nor structural irregularity. Nevertheless, these conclusions have not been verified by experimental results in their works. Till now, the reported

experimental data are rare and almost provided by the foam manufacturers [1], who have not discussed the impacts of different factors in their reports. In this work, LTEC of the closed-cell aluminum foams of different density was measured in the temperature range of 100–500 °C, and the effects of density, temperature, composition, residual stress and phase transition were discussed. Particularly, anomalies due to residual stress and phase transition have been found and experimentally analyzed.

2 Experimental

2.1 Material

The closed-cell aluminum foam used in this work was manufactured in a similar way to that of Alporas (Shinko Wire) foam [23]. The relative density ρ_r is defined as the ratio of the density of the foam to that of the base material. In this work, the density of the base material was set as that of the pure aluminum, 2.7 g/cm^3. The samples were machined with wire-electrode cutting facility.

2.2 Linear thermal expansion coefficient

The LTEC was measured with a high-temperature horizontal-type dilatometer. The size of the sample was 10 mm × 10 mm × 50 mm. In a quartz tube, the sample was held with one end contacting a testing rod. The testing rod was joined with a displacement transducer which had a resolution of 1 μm. As the end of the rod was flat and larger than the pores of the foam, the rod would not sink into the pores to induce error during the test. The entire quartz tube was located in an electric heating furnace with a temperature-control chip. The furnace temperature was measured with a K-type thermocouple attached to the quartz tube near the sample. The precision of the furnace temperature measurement was ±1 °C. Due to good thermal insulation of the furnace, it was ensured that the sample has the same temperature as that of the furnace. The average LTEC $\bar{\alpha}$ was determined as

$$\bar{\alpha} = \frac{\Delta L(T) - K(T)}{L_0 \cdot (T - T_0)}. \tag{1}$$

The initial length of the sample L_0 was measured with a vernier caliper. T_0 was the initial temperature of the sample, i.e., the room temperature. As the testing system also thermally expanded during the experiment, the measured length change $\Delta L = L - L_0$ should be modified. The modification quantity $K(T)$ was calibrated by testing an Al_2O_3 sample of known LTEC. During the test, the furnace was first heated to 500 °C at the rate of 5 °C/min, and then cooled naturally. The length change and temperature of the sample were recorded during both the heating and cooling processes. Each sample was tested 4 times.

By taking the logarithm and differential of Eq. (1) successively, one can obtain the following equations:

$$\ln \bar{\alpha} = \ln(\Delta L(T) - K(T)) - \ln L_0 - \ln(T - T_0), \tag{2a}$$

$$\frac{\mathrm{d}\bar{\alpha}}{\bar{\alpha}} = \frac{\mathrm{d}\Delta L(T)}{\Delta L(T) - K(T)} - \frac{\mathrm{d}K(T)}{\Delta L(T) - K(T)} - \frac{\mathrm{d}L_0}{L_0} - \frac{\mathrm{d}T}{T - T_0} + \frac{\mathrm{d}T_0}{T - T_0}. \tag{2b}$$

Then, the uncertainty of the average LTEC can be calculated as

$$\frac{U_{\bar{\alpha}}}{\bar{\alpha}} = \sqrt{\left(\frac{U_{\Delta L}}{\Delta L(T)\text{-}K(T)}\right)^2 + \left(\frac{U_{K(T)}}{\Delta L(T)\text{-}K(T)}\right)^2 + \left(\frac{U_{L_0}}{L_0}\right)^2 + \left(\frac{U_T}{T - T_0}\right)^2 + \left(\frac{U_{T_0}}{T - T_0}\right)^2}. \tag{3}$$

$U_{\Delta L}$ and U_{L_0} were 0.001 and 0.02 mm, respectively. U_T and U_{T_0} could be taken as 1 °C. In extreme cases, the uncertainty of $K(T)$ was assumed to be 100 %, i.e., $U_{K(T)} = K(T)$. According to the experimental data, $U_{K(T)}/(\Delta L - K(T))$ was the main uncertainty term, which decreases with temperature. Finally, the experimental uncertainty of the average LTEC was found to be between 3 % and 6 %.

2.3 Other analyses

In order to study the effects of composition, residual stress and phase transition on LTEC, the closed-cell aluminum foam was tested with XRF, XRD and DSC.

XRF-1800 (Shimadzu) was used to analyze the elemental composition. The samples were thin circular plate obtained by compressing the bulk foam and tested in vacuum at room temperature.

XRD analysis was achieved with X'Pert (PANalytical), using CuK_{α_1} (wavelength: 0.15406 nm) and CuK_{α_2} (wavelength: 0.15443 nm) X-rays. The samples were powder obtained by grinding the foams and tested during two heating/cooling thermal cycles in vacuum. The measurement temperature points were 25, 100, 200, 300, 400 and 500 °C. The interplanar spacings were calculated according to the Bragg equation:

$$2d \sin\theta = \lambda, \tag{4}$$

where d, θ and λ are interplanar spacing, diffraction angle and wavelength of CuK_{α_1} X-ray, respectively. Using the similar treatment of Eq. (1), the uncertainty of d can be calculated as:

$$\frac{U_d}{d} = U_\theta \cot\theta. \quad (5)$$

Equation (5) shows that the error of d can be significantly large when θ is small. U_θ was estimated to be 0.02° in this work, and U_d/d was found to be less than 0.04 %.

DSC analysis was done with Q2000 (TA Instruments) in the temperature range of 100–500 °C. Samples were tested twice with general DSC analysis, at heating/cooling rates of 10 °C/min. With the sapphire reference, the specific heat was quantitatively measured. All the samples were cut from the adjacent positions of the LTEC samples and were washed in an ultrasonic cleaning machine successively with acetone, alcohol and deionized water. In order to exclude the effect of contaminant, DSC–TGA (thermogravimetric analysis) of the wire-electrode cutting oil was tested with SDT Q600 (TA Instruments). All the measurements were done in nitrogen atmosphere.

3 Results and discussion

A total of 20 samples were made from the same batch of the closed-cell aluminum foam, with a relative density range of 0.096–0.211. The samples were numbered from 1 to 20 in density-increasing order. For comparison, a pure aluminum sample (99.3 wt% Al) was made and tested. For brevity, the following discussions are mainly limited to Sample 1 ($\rho_r = 0.096$) and Sample 15 ($\rho_r = 0.163$), whereas all the methods and conclusions apply to the rest samples. Notably, all the phenomena discussed in the following parts were confirmed with the results of dilatometer TMA Q400 (TA Instruments).

3.1 Effects of the density and composition

The average LTECs over the temperature range of 20–500 °C are plotted in Fig. 1. The results of the pure aluminum during the third and fourth tests are the same, thus presented with one shared curve. As the tests are repeated, average LTECs of both the foams and the pure aluminum increase to their stable values, which are in the same varying range. Except the results of the first experiment, the measured LTECs of the foam coincide well with the reported values listed in Table 1 [1].

Almanza et al. [24] pointed out that the following equation applies to all kinds of closed-cell foams:

$$\alpha_F = \alpha_M + (\alpha_A - \alpha_M)\frac{K_A}{K_F}, \quad (6)$$

where α is LTEC, and K is bulk modulus. Subscripts F, M and A denote the foam, solid matrix and internal air, respectively. For ideal gas, α_A equals to $1/(3T^*)$, where T^* is the absolute temperature. K_A equals to gas pressure, while K_F depends on the density and internal structure of the foam. As for closed-cell aluminum foam, K_A (around 0.1 MPa) is far less than K_F (around 1,000 MPa). Therefore, the second term on the right side of Eq. (6) can be ignored, leading to $\alpha_F = \alpha_M$. So it can be concluded that LTEC of the closed-cell aluminum foam is the same as that of the cell wall material, thus independent of its relative density. This result has experimentally validated the similar conclusions obtained by Kitazono et al. [21] and Hosseini et al. [22] through simulation. As listed in Table 2, the content of Al in the foams used in this work is more than 85 wt%, so the LTEC of foams are close to that of the pure aluminum. However, a considerable amount of Ca, Fe and Ti exist in the foams in addition to Al.

3.2 Effect of the residual stress

Figure 1 shows that the LTECs of the foams vary in a wide range in the first experiment. The details of the sample length change during the tests are listed in Table 3. After each test, the net length change is always negative, implying that the samples become shorter. The largest net length change occurs in the first test. As the tests are repeated, the net length change approaches to zero. It

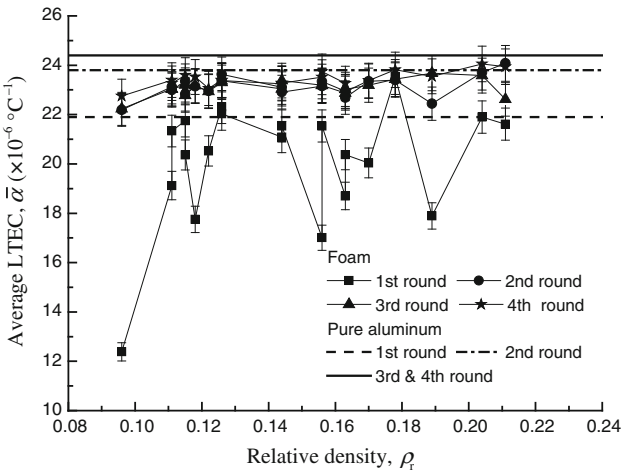

Fig. 1 Average LTEC of the closed-cell aluminum foams and pure aluminum (from 20 to 500 °C)

Table 1 Reported average LTEC of aluminum foams [1]

Category	Cymat	Alulight	Alporas	ERG
Solid material	Al–SiC	Al	Al	Al
Cell type	Closed	Closed	Closed	Open
$\bar{\alpha}$ (10^{-6} °C^{-1})	19–21	19–23	21–23	22–24

Table 2 Elemental composition of the closed-cell aluminum foams measured with XRF (wt%)

Sample	Al	Ca	Fe	Ti
1	85.50	8.65	2.29	1.70
15	90.09	5.19	2.95	0.95

Table 3 Length change $L - L_0$ during the LTEC tests (μm)

ρ_r	Number of test	100 °C→500 °C	500 °C→100 °C	Net change
0.096 (Sample 1)	First	+224	−489	−265
	Second	+452	−474	−22
	Third	+457	−470	−13
	Fourth	+463	−470	−7
0.163 (Sample 15)	First	+414	−481	−67
	Second	+466	−477	−11
	Third	+472	−476	−4
	Fourth	+472	−477	−5

should be noted that the length changes during all the cooling processes are almost stable, while the length change during the heating processes increases with the number of tests, and finally tends to be the same as that during the cooling processes.

As shown in Table 3, the length change during the heating/cooling process is around 1 % of sample length (50 mm), so the instantaneous LTEC can be deduced as:

$$\alpha(T)=\frac{1}{L(T)}\frac{\mathrm{d}L(T)}{\mathrm{d}T}\approx\frac{1}{L_0}\frac{\mathrm{d}L(T)}{\mathrm{d}T}. \quad (7)$$

By polynomial fitting and differentiating the measured length, the term $\mathrm{d}L(T)/\mathrm{d}T$ can be calculated. By doing so, instantaneous LTEC curves are obtained as shown in Fig. 2. It can be seen that thermal expansion behavior is nearly the same during the cooling processes, but varies during the heating processes. During the first heating process, instantaneous LTEC declines in the range of 200–400 °C. Particularly, Sample 1 even shows negative instantaneous LTEC in the first heating process.

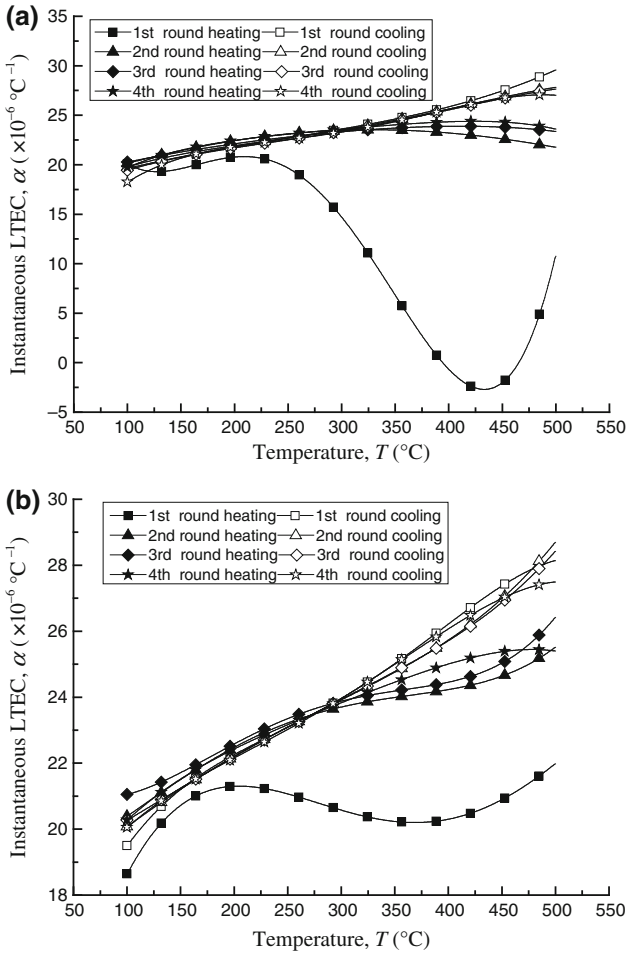

Fig. 2 Instantaneous LTEC curves of the closed-cell aluminum foams. **a** Sample 1; **b** Sample 15

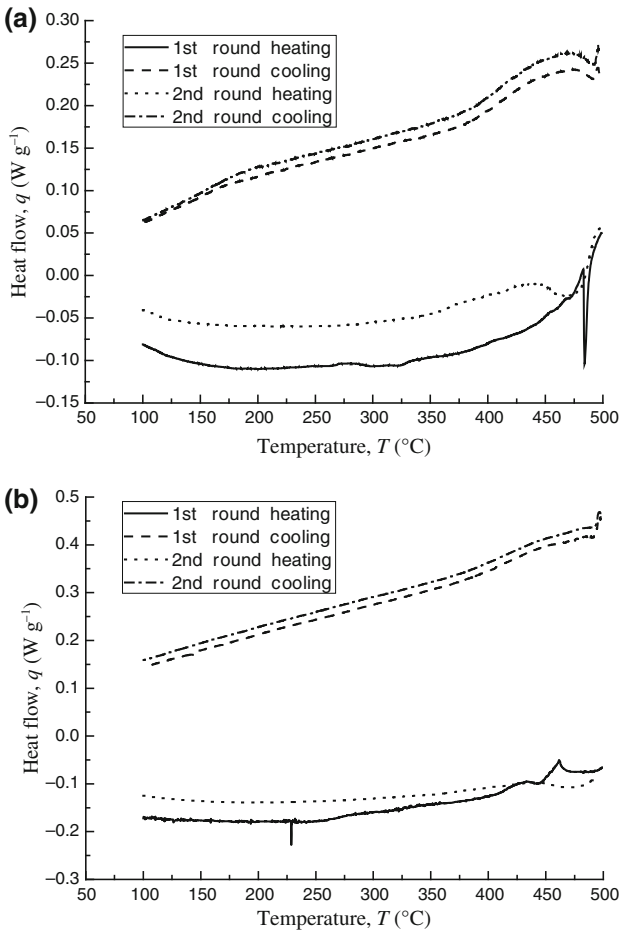

Fig. 3 General DSC results of the closed-cell aluminum foams. **a** Sample 1; **b** Sample 15

Residual stress and phase transition can lead to such decrease of the LTEC in the aluminum alloy or composite [25, 26]. In order to check whether phase transition occurs during the LTEC tests, thermal analyses were done on the closed-cell aluminum foams. The results of the general DSC analysis are shown in Fig. 3. It should be noted that the burrs on the curves result from the oil contaminant introduced in the wire-electrode cutting process, because associated phenomenon can be observed on the DSC–TGA curves of the oil. The endothermic peaks at 484 °C of Sample 1 and 232 °C of Sample 15 are caused by volatilization or decomposition of the oil. In the temperature range where instantaneous LTEC declines in the first heating process (Fig. 2), no phase transition occurs.

The XRD results of Sample 1 and Sample 15 are the same, so only the results of Sample 1 are shown in Fig. 4. For clarity, results at intermediate temperatures are not shown. It can be seen that the cell wall material consists of phase Al (ICDD PDF 04-0787), Al_4Ca (ICDD PDF 14-0428) and $Ti_2Al_{20}Ca$ (ICDD PDF 51-1056). This result is coherent with that of compositional analysis and electron microscopy by Simone et al. [27] and Byakova et al. [28]. The peak broaden effect attenuates during the first heating process, which is represented by the ramification of Al

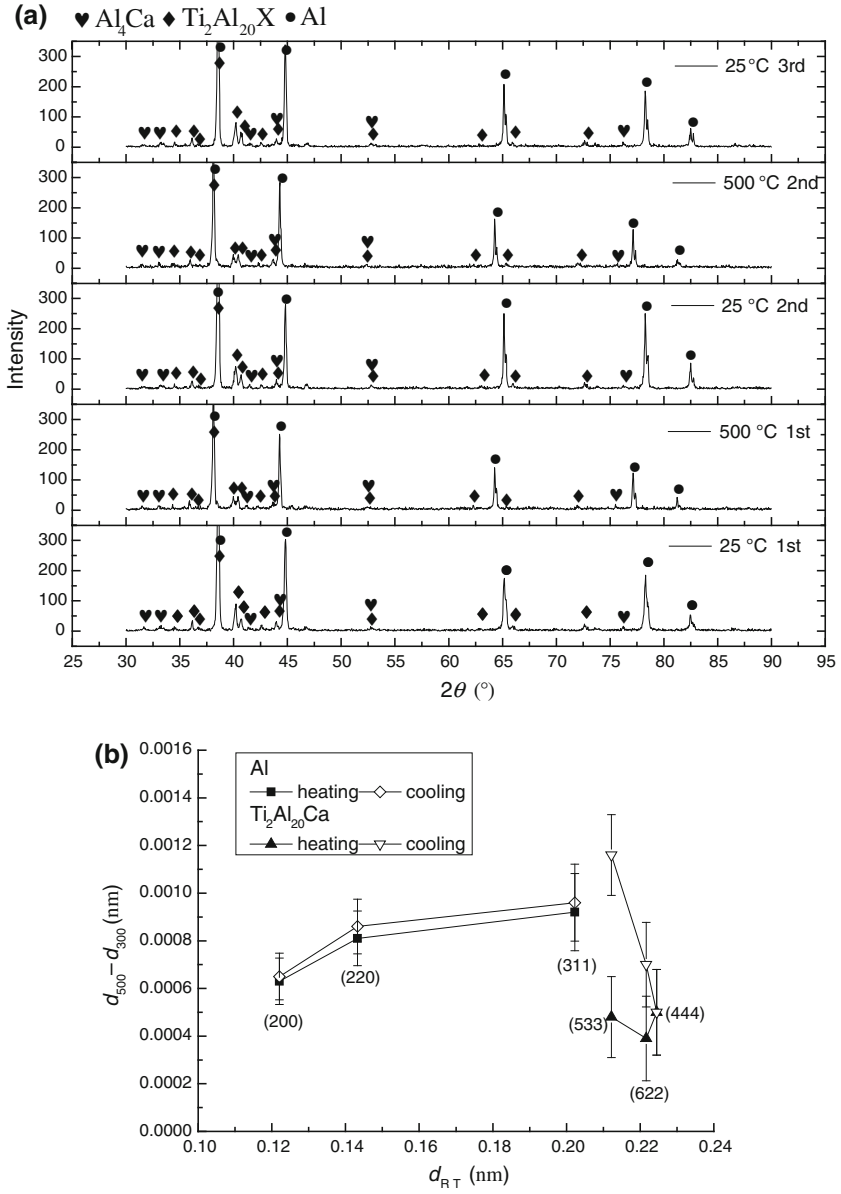

Fig. 4 XRD results of the closed-cell aluminum foams. **a** XRD patterns; **b** difference in interplanar spacings of Al and $Ti_2Al_{20}Ca$ between 300 and 500 °C

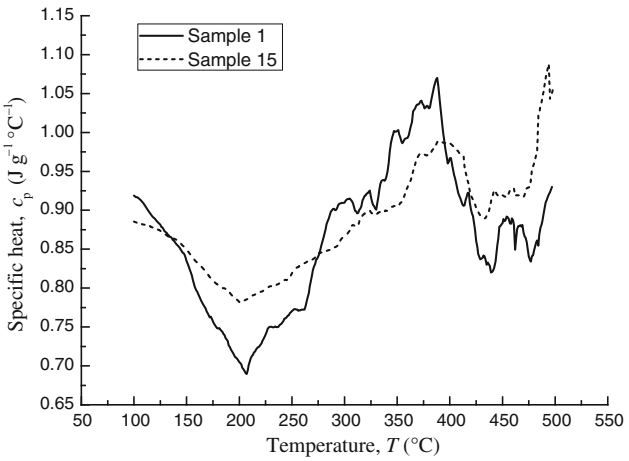

Fig. 5 Specific heat of the closed-cell aluminum foams

peaks at large θ positions. The ramification is in fact the distinguished diffraction peaks of CuK_{α_1} and CuK_{α_2} X-rays, which means that fluctuation of interplanar spacing becomes weak. In the present case, the ramification should result from the release of the residual stress.

In conclusion, the decrease of the LTEC in the first heating process results from the release of the residual stress. As the samples become shorter after the tests, the residual stress should be tensile stress.

3.3 Effect of the phase transition

As shown in Fig. 2, thermal expansion property becomes stable after several repeated tests. It is worthy noting that beyond 300 °C, instantaneous LTEC during the heating process is always lower than that during the cooling process. This hysteresis is an implication of phase transition [29]. When the temperature reaches 400 °C, the DSC curves of the foams exhibit characteristics of a second-order phase transition [30] as shown in Fig. 3. Furthermore, Fig. 5 shows that the specific heat of the foams does reach a maximum in the temperature range of 300–450 °C, which confirms the second-order phase transition [29].

Interestingly, similar hysteresis of the LTEC [31] and maximum of the specific heat [32] were detected in the Nb-H hydride around 390 K. Such phenomena have been found to be related to the order-disorder phase transition [32, 33], which results from the change of the hydrogen distribution in the Nb crystal lattice. Such change also happens in the $LaNi_{4.78}Sn_{0.22}D_x$ hydride [34]. The hydrogen atoms redistribute in the lattice during desorption, leading to a sudden contract of the lattice size in certain direction [34]. As no hydrogen redistribution occurs during absorption, such contract is irreversible [34].

XRD patterns in Fig. 4a show that throughout 25–500 °C, the characteristic lattice structures of Al, $Ti_2Al_{20}Ca$ and Al_4Ca always exist and no new phase emerges. However, it should be noted that XRD has difficulty in directly detecting hydrogen distribution in the hydride [35], especially when the presence of hydrogen does not change the lattice type of the host metal. Considering the blowing agent TiH_2 used in the foaming and the results of literature [32, 34], the second-order phase transition in the foams probably results from the redistribution of some residual hydrogen. In other words, $Al/Ti_2Al_{20}Ca/Al_4Ca$ and the residual hydrogen may compose certain metal hydride.

In order to confirm such presumption, the interplanar spacings of each phase are analyzed based on the data of XRD. According to the results of the LTEC and specific heat, the phase transition occurs beyond 300 °C. So the interplanar spacings of the main crystal planes of each phase at 300 and 500 °C are calculated and denoted as d_{300} and d_{500}, respectively. Together with the index (*hkl*), the room temperature spacing d_{RT} is used to label the corresponding crystal plane. The difference $d_{500} - d_{300}$ can represent the length change of each phase as shown in Fig. 4b. The $d_{500} - d_{300}$ of each crystal plane in Al are nearly the same for heating and cooling processes, which means Al phase is not involved in the phase transition. While for (533) and (622) planes of $Ti_2Al_{20}Ca$, $d_{500} - d_{300}$ during heating process is significantly lower than that during cooling process, which is consistent with the hysteresis of the instantaneous LTEC. The interplanar spacings of Al_4Ca are hard to be accurately measured, because the content is low and the main diffraction peaks are located in the low θ range (Fig. 4a). However, the content of Al_4Ca is so low that it cannot be the dominant phase of the phase transition even if it is involved.

In conclusion, the hysteresis of the instantaneous LTEC should result from the redistribution of some residual hydrogen in the lattice of $Ti_2Al_{20}Ca$, which causes significant lattice contract during the heating process.

4 Conclusions

In summary, the effects of relative density, composition, residual stress and phase transition on the LTEC of the closed-cell aluminum foams have been discussed in the temperature range of 100–500 °C. The cell wall material of the closed-cell foams mainly consists of Al, Al_4Ca and $Ti_2Al_{20}Ca$ phase. The LTEC of the closed-cell aluminum foam is close to that of the pure aluminum, mainly dominated by the properties of the cell wall material, and independent on the relative density. In the first heating process, as most of the residual tensile stress is released, the LTEC declines significantly and even shows negative values. As the tests are repeated, all residual stress can be released. With temperature higher than 300 °C, the

instantaneous LTEC shows hysteresis, which should result from the redistribution of some residual hydrogen in the $Ti_2Al_{20}Ca$ lattice, causing significant lattice contract during the heating process.

Acknowledgments This work was supported by the National Natural Science Foundation of China (90916026). The authors would like to thank Guien Zhou, Guanyin Gao, Yanwei Ding and Shiding Zhang for their supports in the XRD, DSC and XRF analyses.

References

1. Ashby MF, Evans T, Fleck NA et al (2000) Metal foams: a design guide. Butterworth-Heinemann, UK
2. Banhart J (2001) Manufacture, characterisation and application of cellular metals and metal foams. Prog Mater Sci 46:559–632
3. Lu TJ, Zhang QC (2009) Development of multifunctional lightweight cellular metals through interdisciplinary efforts. Chin Sci Bull 54:3844–3846
4. Nieh TG, Higashi K, Wadsworth J (2000) Effect of cell morphology on the compressive properties of open-cell aluminum foams. Mat Sci Eng A Struct 283:105–110
5. Lu TJ, Ong JM (2001) Characterization of close-celled cellular aluminum alloys. J Mater Sci 36:2773–2786
6. Markaki AE, Clyne TW (2001) The effect of cell wall microstructure on the deformation and fracture of aluminium-based foams. Acta Mater 49:1677–1686
7. Benouali AH, Froyen L, Dillard T et al (2005) Investigation on the influence of cell shape anisotropy on the mechanical performance of closed cell aluminium foams using micro-computed tomography. J Mater Sci 40:5801–5811
8. Raj RE, Daniel BSS (2009) Structural and compressive property correlation of closed-cell aluminum foam. J Alloy Compd 467:550–556
9. Onck P, Van Merkerk R, Raaijmakers A et al (2005) Fracture of open- and closed-cell metal foams. J Mater Sci 40:5821–5828
10. Jeon I, Katou K, Sonoda T et al (2009) Cell wall mechanical properties of closed-cell Al foam. Mech Mater 41:60–73
11. Lu TJ, Chen C (1999) Thermal transport and fire retardance properties of cellular aluminium alloys. Acta Mater 47:1469–1485
12. Coquard R, Baillis D (2009) Numerical investigation of conductive heat transfer in high-porosity foams. Acta Mater 57:5466–5479
13. Fiedler T, Solórzano E, Garcia-Moreno F et al (2009) Lattice Monte Carlo and experimental analyses of the thermal conductivity of random-shaped cellular aluminum. Adv Eng Mater 11:843–847
14. Fiedler T, Solórzano E, Garcia-Moreno F et al (2009) Computed tomography based finite element analysis of the thermal properties of cellular aluminium. Materialwiss Werkst 40:139–143
15. Veyhl C, Belova IV, Murch GE et al (2011) Thermal analysis of aluminium foam based on micro-computed tomography. Materialwiss Werkst 42:350–355
16. Paek JW, Kang BH, Kim SY et al (2000) Effective thermal conductivity and permeability of aluminum foam materials. Int J Thermophys 21:453–464
17. Babcsan N, Meszaros I, Hegman N (2003) Thermal and electrical conductivity measurements on aluminum foams. Materialwiss Werkst 34:391–394
18. Solorzano E, Rodriguez-Perez MA, Reglero JA et al (2007) Density gradients in aluminium foams: characterisation by computed tomography and measurements of the effective thermal conductivity. J Mater Sci 42:2557–2564
19. Sadeghi E, Hsieh S, Bahrami M (2011) Thermal conductivity and contact resistance of metal foams. J Phys D Appl Phys 44:125406–125412
20. Lázaro J, Escudero J, Solórzano E et al (2009) Heat transport in closed cell aluminum foams: application notes. Adv Eng Mater 11:825–831
21. Kitazono K, Sato E, Kuribayashi K (2003) Application of mean-field approximation to elastic-plastic behavior for closed-cell metal foams. Acta Mater 51:4823–4836
22. Hosseini SMH, Kharaghani A, Kirsch C et al (2011) Numerical investigation of the thermal properties of irregular foam structures. In: Ochsner A, Murch GE, Delgado JMP (eds) Diffusion in solids and liquids Vi, Pts 1 and 2, vol 312–315. Trans Tech Publications, Switzerland, pp 941–946
23. Miyoshi T, Itoh M, Akiyama S et al (2000) ALPORAS aluminum foam: production process, properties, and applications. Adv Eng Mater 2:179–183
24. Almanza O, Masso-Moreu Y, Mills NJ et al (2004) Thermal expansion coefficient and bulk modulus of polyethylene closed-cell foams. J Polym Sci Pol Phys 42:3741–3749
25. Huang YD, Hort N, Dieringa H et al (2005) Analysis of instantaneous thermal expansion coefficient curve during thermal cycling in short fiber reinforced $AlSi_{12}CuMgNi$ composites. Compos Sci Technol 65:137–147
26. Chen N, Zhang H, Gu M et al (2009) Effect of thermal cycling on the expansion behavior of Al/SiC_p composite. J Mater Process Tech 209:1471–1476
27. Simone AE, Gibson LJ (1998) Aluminum foams produced by liquid-state processes. Acta Mater 46:3109–3123
28. Byakova A, Gnyloskurenko S, Nakamura T (2012) The role of foaming agent and processing route in the mechanical performance of fabricated aluminum foams. Metals 2:95–112
29. Wang R (1985) Physical properties of metal materials. Metallurgical Industry Press, Beijing
30. Lu XS (1990) Phase diagram and phase transition. USTC Press, Hefei
31. Sorokina NI, Wlocewicz D, Plackowcki T (1996) Phase transitions in Nb-H system. Int J Hydrog Energy 21:939–943
32. Plackowski T, Sorokina NI, Wlosewicz D (1998) Order-disorder phase transitions in $NbH_{0.86}$. J Phys-condens Mat 10:1259
33. Welter JM, Schondube F (1983) A resistometric and neutron diffraction investigation of the Nb-H system at high hydrogen concentrations. J Phys F Metal Phys 13:529
34. Nakamura Y, Bowman RC Jr, Akiba E (2007) Variation of hydrogen occupation in $LaNi_{4.78}Sn_{0.22}D_x$ along the P-C isotherms studied by in situ neutron powder diffraction. J Alloy Compd 431:148–154
35. Bau R, Teller RG, Kirtley SW et al (1979) Structures of transition-metal hydride complexes. Acc Chem Res 12:176–183